JOURNAL OF GUIDANCE, CONTROL, AND DYNAMICS
Vol. 34, No. 1, January–February 2011

Reference Management for Fault-Tolerant Model Predictive Control

Fabio A. de Almeida*
Grupo Especial de Ensaios em Voo, 12228-904 São José dos Campos, Brazil

DOI: 10.2514/1.50938

This work presents a reference management technique for fault-tolerant model predictive control. The reference value to be tracked is first filtered through a set of statically admissible commands. This set expresses the airframe's physical ability to achieve a new equilibrium point, and it is constructed by considering the limitations of the inputs and states of the system under control. The set has a polyhedral form defined by linear inequalities. State and control vectors are obtained at steady state to guarantee the feasibility of the constrained numerical problem faced by the model predictive control regulator. The proposed method has been evaluated using a linear model of a fighter aircraft, and it demonstrated adequate performance with a computational burden compatible with real-time applications.

Nomenclature

A, B, C	=	continuous-time state-space matrices
A_m	=	reference state-space matrix
C_c	=	output constraint matrix
C_N	=	stacked correction vectors
c	=	correction vector
$d_{\max}$, $d_{\min}$	=	bounds over disturbance vector
E	=	observation matrix
E_a	=	augmented observation matrix
e	=	model following error
H	=	tracking matrix
I	=	identity matrix
J	=	cost function
K_d	=	feedback gain matrix
k_{ss}, k_N	=	linear inequalities vectors
L, L_d, L_x	=	observer gain matrices
$\bar{L}_d$, $\bar{H}$	=	auxiliary observer matrices
L_{ss}, M_x, $M_{x_{ss}}$, $M_{u_{ss}}$, M_d	=	linear inequalities matrices
N	=	control horizon
O_∞	=	invariant set
$\tilde{O}_\infty$	=	tracking invariant set
P	=	terminal weighting matrix
$\mathbf{P}_m$	=	set of statically admissible commands given the current disturbance
$\mathbf{P}_{ss}$	=	steady-state polyhedron
$\mathbf{P}_w$	=	set of statically admissible commands
p, q, r	=	aircraft angular rates, rad/s
Q, W, R	=	weighting matrices
Q_d, W_d, R_d	=	discrete weighting matrices
Q_m, W_m, R_m	=	implicit model following weighting matrices
Q_{ss}, R_{ss}	=	constrained target calculator weighting matrices
r_c	=	command (demand) vector
r_{ss}	=	statically admissible command vector
T	=	rotation matrix
T_s	=	sampling time, s
t	=	time, s
$u_{\max}$, $u_{\min}$	=	bounds over control vector
w	=	performance output vector
w_m	=	reference model state vector
$\mathbf{X}$, $\mathbf{U}$	=	admissible state and control sets
$\mathbf{X}_N$	=	set of admissible extended state vectors
$\mathbf{X}_{ss_N}$	=	set of admissible steady-state control and state vectors
x, u	=	state and control vectors
x_a	=	augmented state vector
$x_{\max}$, $x_{\min}$	=	bounds over state vector
x_{ss}, u_{ss}	=	state and control vectors at steady state
x_0	=	initial state vector
$\hat{x}$, $\hat{d}$	=	estimated state and disturbance vectors
$\tilde{x}$, $\tilde{u}$	=	tracking state and control vectors
y	=	observed vector
z	=	controlled output vector
z_{ss}	=	feasible command vector
α, β	=	angles of attack and sideslip, rad
δ_c, δ_r	=	canard and rudder deflections, rad
δ_{r_e}, δ_{l_e}	=	right and left elevon deflections, rad
ϵ_x, ϵ_z	=	tolerance vectors
π	=	projection operator
σ	=	slice operator
Φ, Γ, Γ_d	=	discrete-time state-space matrices
$\bar{\Phi}$	=	auxiliary discrete state-space matrix
Φ_a, Γ_a	=	augmented discrete state-space matrices

I. Introduction

MODERN fault-tolerant flight control systems may possess the capability to redistribute the control effort among healthy actuators, given that the control system has some degree of redundancy. In the event of structural or actuator fault, the fault-tolerant control must isolate the fault and reallocate the reference commands in a manner that achieves the control objectives, minimizing the impact of the fault in the performance and flying qualities of the aircraft.

Several techniques that perform control redistribution in aerospace applications are currently available. However, few of them are able to determine whether a certain reference command is physically achievable or not. Depending on the severity of the fault, the maneuverability of the aircraft can be seriously compromised, to the point that some states would not be reachable and certain commands could not be followed. Even the task to return home safely may become impossible. Moreover, the static capabilities of the faulty aircraft are not the only important considerations, but the dynamic capabilities of the controller to steer states from one equilibrium

Presented as Paper 2010-7704 at the AIAA Guidance, Navigation, and Control Conference, Toronto, Canada, 2–5 August 2010; received 27 May 2010; revision received 1 October 2010; accepted for publication 1 October 2010.

*Flight Test Instructor, Escola de Formação em Ensaios em Voo, Pça Marechal Eduardo Gomes 50. Senior Member AIAA.

point to another, without violating constraints, even in the presence of external disturbances must be considered. Thus, the reference command must also be filtered to account for the current state of the aircraft and its limitations. In other words, a fault-tolerant controller must take into account the admissibility and feasibility of the reference commands. The former aspect is concerned with the set of states and references achievable by a faulty airframe. The second aspect, also related to stability, is critical when severe constraints and aggressive demands must be handled by the constrained controller.

In the last decade, the problem of determining the statically admissible set of reference command values for a vehicle with faulty actuators has gained some attention in the literature. Strube et al. [1] proposed the creation of a database for different fault conditions with related achievable trim conditions, which could be employed by outer control loops. Ducard et al. [2] has evaluated the reduced performance of an unmanned aerial vehicle after an aileron failure in terms of admissible bank angles and time to roll to the limiting angle.

In addition to the research effort in reference management for fault-tolerant control systems, the topic of constrained control presents some solutions to this problem, specifically through dynamic filtering of the reference level in the presence of saturated actuators. Since the seminal work of Kapasouris et al. [3], several works have proposed solutions to implement dynamic demand shaping. Gilbert and Tan [4] proposed a command governor to adjust the tracking error, and avoid saturation of the system inputs and/or outputs. This concept has been further developed [5], combined with disturbance models [6], and extended to linear time-variant [7] and nonlinear systems [8,9]. Recently, Famularo et al. [10] developed a flight control system with envelope protection capabilities based on the command governor approach. Following the concept of reference management, Zhang and Jiang [11] propose an input command management system to adjust infeasible demands to the fault-tolerant control.

Another important technique for controlling constrained systems is model predictive control (MPC). Basically, MPC is an optimal control technique, generally with the same cost function as the well-known linear quadratic regulator (LQR). The basic difference is the introduction of constraints in the inputs, states, and output of the plant. Recent works [12–15] have demonstrated the possibilities of using MPC to perform control redistribution in the event of failures simply by changing the constraints of the faulty actuator. Additionally, Chisci and Zappa [16] shows that MPC combined with a command governor device can substantially improve the controller's domain of operation. Recently, Limon et al. proposed nominal [17] and robust [18] formulations of MPC with demand filtering to guarantee stability and feasibility. However, in those formulations the sets of constraints on the states and inputs must necessarily contain the origin, restricting its application in the scope of fault-tolerant control systems.

Therefore, considering the current limitations of MPC and fault-tolerant controllers, this work proposes a novel reference management method for MPC. This formulation combines the method of calculating the set of statically admissible demands to a constrained control system [15] with the technique called feasible target-tracking MPC [19]. The complete control system is capable of filtering, in both static and dynamic ways, the reference value to be followed given input and/or output constraints. The reference command is first checked to see whether it corresponds to a new equilibrium point or not. The reference is then filtered again, to guarantee the feasibility of the constrained optimization problem. Simulation results using the linear model of the ADMIRE aircraft under severe fault scenarios are provided and demonstrate adequate performance of the controller while also requiring shorter control horizons than current MPC formulations.

The proposed reference management method relies on projection algorithms, numerical techniques with growing importance in control applications, particularly in applications with polyhedral constraints. Several techniques are available, including Fourier–Motzkin elimination, equality set projection and vertex enumeration. A comprehensive review of these techniques is provided by Jones et al. [20].

This paper is organized as follows: first, the technique to obtain the set of statically admissible commands is presented. Then, the feasible target-tracking MPC method is presented. Finally, simulation results using the fault-tolerant MPC with static and dynamic filtering are shown and discussed.

II. Set of Statically Admissible Commands

Let the discrete-time state-space model be defined by

$$x_{k+1} = \Phi x_k + \Gamma u_k + \Gamma_d d_k \qquad d_{k+1} = d_k$$
$$y_k = E x_k \qquad z_k = H y_k \tag{1}$$

where $x_k \in \mathbb{R}^n$ is the state vector, $u_k \in \mathbb{R}^m$ is the control vector, $y_k \in \mathbb{R}^p$ is the vector of observed variables, $d_k \in \mathbb{R}^q$ is the vector of disturbances and $z_k \in \mathbb{R}^q$, $q \le m$, is the vector of controlled variables. The disturbance vector is included to model mismatches between the plant and the nominal model as well as external disturbances acting on the plant. The pair (E, Φ) is assumed to be detectable with E full row rank. Additionally, the disturbance vector is assumed to be estimated by a proper observer. In this work, the disturbance model is simply a constant value.

The objective of the control system is to asymptotically eliminate the tracking error given a reference command r_{ss}, that is,

$$z_k \underset{k\to\infty}{\rightarrow} r_{ss} \tag{2}$$

in the presence of a disturbance d_k and given constraints on the state and control vectors $x_k \in \mathbf{X}$, $u_k \in \mathbf{U}$, where $\mathbf{X}$ and $\mathbf{U}$ are closed, bounded and convex sets expressed by linear inequalities. This problem corresponds to finding a new equilibrium point for the plant in steady state, which is essentially a determination of the steady-state target vectors $x_{ss}(r_{ss}, d_k)$ and $u_{ss}(r_{ss}, d_k)$ and is expressed by

$$(\Phi - I)x_{ss} + \Gamma u_{ss} + \Gamma_d d_k = 0$$
$$HEx_{ss} = r_{ss} \qquad u_{ss} \in \mathbf{U} \qquad x_{ss} \in \mathbf{X} \tag{3}$$

In the context of fault-tolerant flight control, it is often the case that constraints are active in steady state, for example, when actuators stuck in a nonzero position or the disturbance d_k is large enough to push states and controls against the constraints. Given that $m \ge q$, the following constrained target calculation problem is solved to obtain x_{ss} and u_{ss}:

$$\min_{x_{ss}, u_{ss}} J(r_{ss}, d_k) = (HEx_{ss} - r_{ss})^T Q_{ss} (HEx_{ss} - r_{ss}) + u_{ss}^T R_{ss} u_{ss}$$
$$\text{subject to: } (\Phi - I)x_{ss} + \Gamma u_{ss} + \Gamma_d d_k = 0$$
$$u_{ss} \in \mathbf{U} \qquad x_{ss} \in \mathbf{X} \tag{4}$$

where Q_{ss} and R_{ss} are weighting matrices.

This problem is solved, at each sampling instant, and the steady-state variables that correspond to the desired output target are obtained. The complete set of attainable steady states and related outputs can be determined by solving Eq. (4) for each pair (r_{ss}, d_k). However, the characterization and construction of this set would be numerically costly, and only approximations to the boundary of the set can be obtained practically. To provide a better, more practical formulation of the attainable set, this section proposes the use of projection algorithms.

Before proceeding with the proposed method, some useful definitions are given. A polyhedron is the intersection of a finite number of closed half-spaces:

$$\mathbf{P} = \{v \in \mathbb{R}^n | L_c v \le k_c\} \tag{5}$$

A polytope is a bounded polyhedron. Given a polyhedron $\mathbf{P} \subset \mathbb{V} \times \mathbb{Y}$, where $\mathbb{V}$ and $\mathbb{Y}$ are subspaces, the projection of $\mathbf{P}$ onto $\mathbb{V}$ is defined as

$$\pi_{\mathbb{V}} \mathbf{P} = \{v \in \mathbb{V} | \exists y \in \mathbb{Y}, (v, y) \in \mathbf{P}\} \tag{6}$$

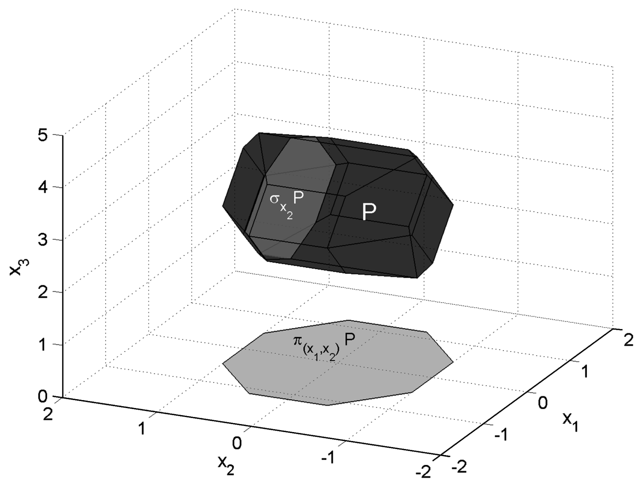

Fig. 1 Projection and slice of a polyhedron.

and the slice of $\mathbf{P}$ at a vector $r \in \mathbb{R}^p$ is defined as

$$\sigma_r \mathbf{P} = \{v \in \mathbb{R}^n | (v, r) \in \mathbf{P}\} \tag{7}$$

Figure 1 illustrates the projection and slice operations in three dimensions. A generic polyhedron $\mathbf{P}$ is projected onto the subspace spanned by dimensions (x_1, x_2). Note that the projection operator reduces the number of spatial dimension. The slice operator is a cut of the polyhedron at a certain value, illustrated in Fig. 1 for a given value of the variable x_2.

The key concept of the proposed technique is the construction of a polyhedron $\mathbf{P}_{ss}$ that corresponds to the constraints imposed in steady state and the projection of $\mathbf{P}_{ss}$ onto a desired subspace. If the performance characteristics at steady state are of interest, a proper subspace can be constructed from the state vector. If maneuverability is the issue under consideration, outputs such as airspeed, flight path angle and turn rate may define another subspace.

The equality constraints represented by the state-space and target equations can be converted into inequality constraints through introduction of an arbitrarily small tolerance vectors ϵ_x and ϵ_z. Hence, Eq. (3) can be rewritten as

$$\begin{aligned}
&(\Phi - I)x_{ss} + \Gamma u_{ss} + \Gamma_d d_k \le \epsilon_x I\\
&(\Phi - I)x_{ss} + \Gamma u_{ss} + \Gamma_d d_k \ge -\epsilon_x I\\
&HEx_{ss} - r_{ss} \le \epsilon_z I\\
&HEx_{ss} - r_{ss} \ge -\epsilon_z I\\
&u_{ss} \in \mathbf{U} \qquad x_{ss} \in \mathbf{X}
\end{aligned} \tag{8}$$

which defines the following polyhedron $\mathbf{P}_{ss}$:

$$\mathbf{P}_{ss} = \{v \in \mathbb{R}^{n+m+2q} | L_{ss} v \le k_{ss}\} \tag{9}$$

where $v = [x_{ss}^T \quad u_{ss}^T \quad r_{ss}^T \quad d_k^T]^T$ and

$$L_{ss} = \begin{bmatrix} C_c & 0 & 0 & 0\\ -C_c & 0 & 0 & 0\\ 0 & I & 0 & 0\\ 0 & -I & 0 & 0\\ 0 & 0 & 0 & I\\ 0 & 0 & 0 & -I\\ \Phi - I & \Gamma & 0 & \Gamma_d\\ -\Phi + I & -\Gamma & 0 & -\Gamma_d\\ HE & 0 & -I & 0\\ -HE & 0 & I & 0 \end{bmatrix}, \qquad k_{ss} = \begin{bmatrix} x_{\max}\\ x_{\min}\\ u_{\max}\\ u_{\min}\\ d_{\max}\\ d_{\min}\\ \epsilon_x\\ -\epsilon_x\\ \epsilon_z\\ -\epsilon_z \end{bmatrix} \tag{10}$$

where $x_{\max}$, $x_{\min}$, $u_{\max}$, $u_{\min}$, $d_{\max}$ and $d_{\min}$ are the bounds of the state, control and disturbance vectors, respectively. The projection of $\mathbf{P}_{ss}$ onto the subspace $\mathbb{W}$ spanned by augmented vectors $[r_{ss}^T \quad d_k^T]^T$ generates a polyhedron $\mathbf{P}_w$ that encodes the maneuverability limitations of the vehicle, provided that the disturbance is known or estimated. The information about the disturbance is crucial because the proposed technique is based on linear models and is generally valid for specific trimmed conditions, so knowledge of the disturbance produces corrections to the assumed model.

It is assumed that the disturbance is available via some observer. Therefore, the limits on r_{ss} are readily calculated by performing the slice operation at the estimated disturbance value. The slice operation is nothing but a simplification of the linear inequalities that define a polyhedron when some variables are known a priori. Thus, the slice results in a polyhedron of reduced dimensionality. The implementation of projection algorithms in real-time applications remains restricted to low-order polyhedra. However, it seems to be useful to determine maneuverability polyhedra offline by assuming different fault combination scenarios that result in different vectors k_{ss}, each of which have different values of $u_{\max}$ and $u_{\min}$. The slice at the estimated disturbance vector is a simple enough operation to be performed in real time.

Therefore, given an actuator fault case, the related maneuverability polyhedron $\mathbf{P}_m$ is obtained through Algorithm 1.

Each fault combination is associated with one polyhedron $\mathbf{P}_m$, which can be easily stored for use in real-time applications because it is represented by only one matrix and one vector. Thus, the admissibility of a given reference r_{ss} is verified by a simple membership operation. Finally, a few considerations pertaining the selected tolerances ϵ_x and ϵ_z are given. Small values of the tolerances are desirable to maintain the integrity of the state and output constraints. However, excessively small tolerances may lead to infeasibility in the projection algorithm, resulting in an empty polyhedron. Hence, it is essential to carefully select these parameters to guarantee the construction of a nonempty maneuverability polyhedron.

III. Feasible Target-Tracking Model Predictive Control

In the last section a technique to determine the set of statically admissible commands was presented. The feasibility of the related quadratic programming (QP) problem is guaranteed through the penalization of difference between the admissible (r_{ss}) and the feasible ($z_{ss} = HEx_{ss}$) targets. Nevertheless, feasibility of the constrained problem does not guarantee feasibility of the constrained MPC regulator because the estimated state and disturbance vectors are not taken into account. For given $\hat{x}_k$ and $\hat{d}_k$, there exists an allowable set of demands that would drive the constrained regulator to a feasible zone, resulting in smaller admissible sets of x_{ss} and u_{ss}. In fact, no assumptions were made with respect to the constrained control system, which is responsible for driving states and controls to the steady-state values. If a MPC strategy is considered, as in the present work, the steady-state values must guarantee the feasibility of the constrained optimization problem.

Based on this requirement, this section presents the feasible target-tracking MPC technique [19] for tracking a desired reference. Feasible target state and control vectors are computed from the values of the state and disturbance vectors and used by the infinite horizon MPC regulator. The weighting matrices of the regulator are selected according to the implicit model following technique [21]. Additionally, a linear observer is proposed to provide offset-free tracking of a time-varying reference [22], which significantly improves the robustness of the controller, especially in cases in which faults cause loss of effectiveness.

Figure 2 shows the overall structure of the solution. The discrete controller (enclosed by the dotted line) has three main functionalities: the feasible target calculation, the MPC optimizer, and a linear observer. It is assumed that a fault detection and isolation system (FDI) provides correct information about the status of the actuators to both the target calculation and MPC schemes.

The feasible target calculation subsystem computes the state and control vectors (x_{ss} and u_{ss}) in steady state, which are required to produce offset-free tracking of the statically admissible reference signal r_{ss}. This calculation considers the limitations of the actuators and the feasibility of the constrained optimization problem.

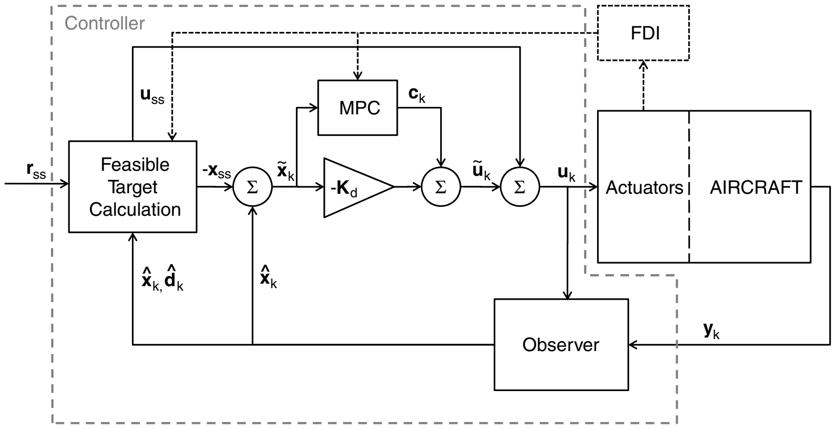

Fig. 2 Overall structure of the feasible target-tracking MPC.

With the calculated steady-state values, the estimated state vector $\hat{x}_k$ is subtracted from x_{ss} to convert the tracking problem into a regulation over the desired steady-state condition. In turn, the regulator control law is the sum of two contributions: a linear part with static linear feedback gain K_d and a nonlinear correction c_k calculated by the MPC system. In the event of an actuator fault, the nonlinear correction c_k redistributes the control effort among the available actuators. A linear, unconstrained observer is employed in the proposed scheme to provide proper estimates of the disturbance $\hat{d}_k$ and the state $\hat{x}_k$.

A. Feasible Target Calculation

The starting point of determining the set is the proposed control law predicted for N steps:

$$\begin{aligned} u_j &= -K_d(x_j - x_{ss}) + u_{ss} + c_j \qquad j = 0, \ldots, N-1 \\ u_j &= -K_d(x_j - x_{ss}) + u_{ss} \qquad j \geq N \end{aligned} \tag{11}$$

where $x_0 = \hat{x}_k$. The MPC regulator calculates the contribution c_j over N steps. It is assumed that after N steps the constraints are no longer active, which is equivalent to saying that the state vector at $j = N$ is inside an invariant set $O_\infty(x_{ss}, u_{ss})$.

Therefore, assuming that x_{ss} and u_{ss} are constant for a given reference, it will be convenient to extend the state-space vector as $[x_j^T \quad x_{ss}^T \quad u_{ss}^T \quad d_j^T]^T$, leading to the following extended dynamic model:

$$\begin{bmatrix} x_{j+1} \\ x_{ss} \\ u_{ss} \\ d_{j+1} \end{bmatrix} = \begin{bmatrix} \Phi - \Gamma K_d & \Gamma K_d & \Gamma & \Gamma_d \\ 0 & I & 0 & 0 \\ 0 & 0 & I & 0 \\ 0 & 0 & 0 & I \end{bmatrix} \begin{bmatrix} x_j \\ x_{ss} \\ u_{ss} \\ d_j \end{bmatrix} + \begin{bmatrix} \Gamma \\ 0 \\ 0 \\ 0 \end{bmatrix} c_j \tag{12}$$

The computation of the invariant set $O_\infty(x_{ss}, u_{ss})$ requires the correct formulation of the constraints that are imposed on $[x_j^T \quad x_{ss}^T \quad u_{ss}^T \quad d_j^T]$. It is clear that the state, input and disturbance constraints can be expressed in terms of linear inequalities:

$$\begin{aligned} &C_c x_j \leq x_{\max} \qquad -C_c x_j \leq -x_{\min} \qquad C_c x_{ss} \leq x_{\max} \\ &-C_c x_{ss} \leq -x_{\min} \qquad u_{ss} \leq u_{\max} \qquad -u_{ss} \leq -u_{\min} \\ &d_j \leq d_{\max} \qquad -d_j \leq -d_{\min} \qquad -K_d x_j + K_d x_{ss} + u_{ss} \leq u_{\max} \\ &K_d x_j - K_d x_{ss} - u_{ss} \leq -u_{\min} \end{aligned} \tag{13}$$

where $x_{\max}, x_{\min}, u_{\min}, u_{\min}, d_{\max}$ and $d_{\min}$ are the bounds on the state, control and disturbance vectors, respectively.

Hence, the set $O_\infty(x_{ss}, u_{ss})$ can be constructed using the techniques described in Gilbert and Tan [4], by considering the extended dynamic system given by Eq. (12) and constraints of Eq. (13). From $O_\infty(x_{ss}, u_{ss})$, one can compute the polyhedral set $\mathbf{X}_N$ of extended states that can be steered to $O_\infty(x_{ss}, u_{ss})$ by N control steps $C_N = \{c_j\}_{j=0}^{N-1}$ while respecting the constraints. This is done by recursion, substituting the dynamic system Eq. (12) into the constraints Eq. (13) for $j = 0, \cdots, N-1$, and then projecting the resulting convex set onto the subspace spanned by $[x_k^T \quad x_{ss}^T \quad u_{ss}^T \quad d_k^T]^T$. The projected polyhedral set $\mathbf{X}_N$ assumes the form

$$\begin{aligned} \mathbf{X}_N = \{(x_k, x_{ss}, u_{ss}, d_k) | M_x x_k + M_{x_{ss}} x_{ss} \\ + M_{u_{ss}} u_{ss} + M_d d_k \leq k_N\} \end{aligned} \tag{14}$$

Finally, the set $\mathbf{X}_{ss_N}$ of admissible steady-state values, which assures the feasibility of the MPC regulator, is computed at each sampling time with the slice operation $\sigma_{(\hat{x}_k, \hat{d}_k)} \mathbf{X}_N$. The computation of $\mathbf{X}_{ss_N}$, for each actuator fault condition, is summarized by Algorithm 2.

The feasible target values of x_{ss} and u_{ss} are obtained through the solution of the QP problem:

$$\begin{aligned} &\min_{x_{ss}, u_{ss}} J(r_{ss}, \hat{x}_k, \hat{d}_k) = (HEx_{ss} - r_{ss})^T Q_{ss} (HEx_{ss} - r_{ss}) + u_{ss}^T R_{ss} u_{ss} \\ &\text{subject to: } (\Phi - I)x_{ss} + \Gamma u_{ss} + \Gamma_d d_k = 0 \\ &(x_{ss}, u_{ss}) \in \mathbf{X}_{ss_N} \end{aligned} \tag{15}$$

It should be noted that $\mathbf{X}_{ss_N} \subseteq \mathbf{X}_{ss_{N+1}}$, because larger control horizons mean more discrete steps to steer the extended state-space into the invariant set $O_\infty(x_{ss}, u_{ss})$. This is equivalent to saying that, for a given pair $(\hat{x}_k, \hat{d}_k)$, the set of feasible steady-state references $z_{ss} = HEx_{ss}$ is wider given larger control horizons.

B. Constrained Implicit Model Following Regulator

The implicit model following form of the MPC regulator [21] was chosen because it provides proper dynamic control allocation when one or more actuators saturate, keeping the transient response as close as possible to the specified reference model.

The objective of the regulator is to drive the state vector to the origin, given $x_0 = x_k$. Defining $\tilde{x}_j = x_j - x_{ss}$ and $\tilde{u}_j = u_j - u_{ss}$, the regulator problem is converted to a tracker by replacing x and u by $\tilde{x}$ and $\tilde{u}$, respectively. The same translation applies to the initial state x_0, the admissible sets $\mathbf{U}$, $\mathbf{X}$, and the invariant set O_∞. This translation cancels the influence of the disturbance on the transient response because $d_k = d_{k+1} = \hat{d}_k$ and then $\tilde{d}_k = 0$. Hence, the discrete-time state-space model for regulation is given by

$$\tilde{x}_{k+1} = \Phi \tilde{x}_k + \Gamma \tilde{u}_k \tag{16}$$

The idea of implicit model following is to modify the continuous-time LQR cost function, penalizing any deviation of the system output from a certain reference model output. Let the continuous-time representation of Eq. (16) be defined by

$$\dot{\tilde{x}} = A\tilde{x} + B\tilde{u} \qquad w = C\tilde{x} \tag{17}$$

Suppose that the performance output w in Eq. (17) follows the transient behavior of the autonomous model:

$$\dot{w}_m = A_m w_m \tag{18}$$

The matrix A_m has the reference eigenstructure of the regulator. When the control objective is met, the performance output w will satisfy Eq. (18). One can define the error by

$$e = \dot{w} - A_m w \tag{19}$$

and a cost function by

$$J = \int_0^\infty (e^T Q e + \tilde{u}^T R \tilde{u})\, \mathrm{d}t \tag{20}$$

Since $\dot{w} = C\dot{\tilde{x}} = CA\tilde{x} + CB\tilde{u}$, the cost function becomes

$$J = \int_0^\infty (\tilde{x}^T Q_m \tilde{x} + 2\tilde{x}^T W_m \tilde{u} + \tilde{u}^T R_m \tilde{u})\, \mathrm{d}t \tag{21}$$

where

$$\begin{aligned} Q_m &= (CA - A_m C)^T Q (CA - A_m C) \\ W_m &= (CA - A_m C)^T QCB \\ R_m &= B^T C^T QCB + R \end{aligned} \tag{22}$$

The equivalent discrete-time version of the performance index of Eq. (21) is an infinite sum over the sampled states and inputs [23]:

$$J = \sum_{j=0}^{\infty} (\tilde{x}_j^T Q_d \tilde{x}_j + 2\tilde{x}_j^T W_d \tilde{u}_j + \tilde{u}_j^T R_d \tilde{u}_j) \tag{23}$$

The discrete versions of the weighting matrices, given a sampling time T_s, are calculated from [24]

$$\begin{aligned} Q_d &= Q_m T_s + (Q_m A + A^T Q_m) T_s^2/2 + \cdots \\ W_d &= W_m T_s + (A^T W_m + Q_m B) T_s^2/2 + \cdots \\ R_d &= R_m T_s + (W_m^T B + B^T W_m) T_s^2/2 + \cdots \end{aligned} \tag{24}$$

where only the first two terms will be used in an approximate determination.

As presented before, the proposed control law given by Eq. (11) defines the stacked vector of control steps $C_N = \{c_j\}_{j=0}^{N-1}$ as the decision variables [25], producing the benefits of controller reconfigurability and numerical stability. Moreover, it is desirable that after N sampling times, the state vector will be inside of a terminal invariant set of the closed-loop system. This terminal constraint will guarantee the stability of the nominal closed-loop system [26]. Therefore, considering the translated sets $\tilde{\mathbf{X}}$, $\tilde{\mathbf{U}}$ and $\tilde{O}_\infty$, the constrained optimal control problem to be solved is given by

$$\begin{aligned} &\min_{\{c_j\}_{j=0}^{N-1}} J(\tilde{x}_0) = \tilde{x}_N^T P \tilde{x}_N + \sum_{j=0}^{N-1} (\tilde{x}_j^T Q_d \tilde{x}_j + 2\tilde{x}_j^T W_d \tilde{u}_j + \tilde{u}_j^T R_d \tilde{u}_j) \\ &\quad \text{subject to: } \tilde{x}_{j+1} = (\Phi - \Gamma K_d)\tilde{x}_j + \Gamma c_j, \qquad \tilde{x}_N \in \tilde{O}_\infty \\ &\quad \tilde{u}_j = -K_d \tilde{x}_j + c_j, \qquad j = 0, \ldots, N-1 \\ &\quad \{\tilde{u}_j\}_{j=0}^{N-1} \in \tilde{\mathbf{U}} \qquad \{\tilde{x}_j\}_{j=0}^{N-1} \in \tilde{\mathbf{X}} \end{aligned} \tag{25}$$

where $\tilde{x}_N^T P \tilde{x}_N = \sum_{j=N}^{\infty} (\tilde{x}_j^T Q_d \tilde{x}_j + 2\tilde{x}_j^T W_d \tilde{u}_j + \tilde{u}_j^T R_d \tilde{u}_j)$ is the cost-to-go function and P is the terminal weight given by the solution of the discrete-time Riccati equation:

$$P = Q_d + \Phi^T P \Phi - (\Phi^T P \Gamma + W_d)(\Gamma^T P \Gamma + R_d)^{-1}(\Gamma^T P \Phi + W_d^T) \tag{26}$$

The feedback gain K_d is given by

$$K_d = (\Gamma^T P \Gamma + R_d)^{-1}(\Gamma^T P \Phi + W_d^T) \tag{27}$$

The conversion of this constrained LQR problem into a QP problem can be found in the literature on MPC [27].

C. Observer for Offset-Free Tracking

In the previous sections perfect knowledge of the state and disturbance vectors was assumed. Because these vectors are not directly measured, an observer must be designed and employed. Consider the augmented plant model obtained from rewriting Eq. (1) as

$$x_{a_{k+1}} = \Phi_a x_{a_k} + \Gamma_a u_k \qquad y_k = E_a x_{a_k} \tag{28}$$

where $x_{a_k} = [x_k^T \quad d_k^T]^T$ and

$$\Phi_a = \begin{bmatrix} \Phi & \Gamma_d \\ 0 & I \end{bmatrix}, \qquad \Gamma_a = \begin{bmatrix} \Gamma \\ 0 \end{bmatrix}, \qquad E_a = [E \quad 0] \tag{29}$$

The proposed linear state/disturbance observer has the form

$$\hat{x}_{a_{k+1}} = \Phi_a \hat{x}_{a_k} + \Gamma_a u_k + L(y_k - E_a \hat{x}_{a_k}) \tag{30}$$

where the estimator gain matrix L is

$$L = \begin{bmatrix} L_x \\ L_d \end{bmatrix} \tag{31}$$

In this work the following sequence is used [22] to construct an observer L:

1) Compute L_x such that $\Phi - L_x E$ is stable and the pair $(\bar{H}E_a, \bar{\Phi})$ is detectable, where

$$\bar{H} = H[E(I - \Phi + \Gamma K_d)^{-1} L_x + I] \qquad \bar{\Phi} = \Phi_a - [L_x^T \quad 0]^T E_a \tag{32}$$

2) Compute $\bar{L}_d$ such that $I - \bar{L}_d \bar{H} E (I - \Phi + L_x E)^{-1} \Gamma_d$ is stable

3) Compute the following matrix:

$$T = \begin{bmatrix} I & -(I - \Phi + L_x E)^{-1} \Gamma_d \\ 0 & I \end{bmatrix} \tag{33}$$

4) Calculate the estimator gain L with

$$L = \begin{bmatrix} L_x \\ 0 \end{bmatrix} + T^{-1} \begin{bmatrix} 0 \\ \bar{L}_d \bar{H} \end{bmatrix} \tag{34}$$

Considering that the reference value r_{ss} lies inside the set of statically admissible commands $\mathbf{P}_m$, this observer design allows constrained offset-free control despite the effects of disturbances and model uncertainty.

IV. Application to Fighter Aircraft

In this section, the application of the reference management strategy presented in Secs. II and III is discussed through a numerical example using the ADMIRE model [28]. ADMIRE (see Fig. 3) is a generic model of a small single-seat fighter aircraft with a delta-canard configuration. It has been extensively used to demonstrate several techniques of fault-tolerant control, because it inherently possesses analytical redundancy [29–31].

The ADMIRE linear model considered in this example has been obtained with Mach 0.22, pressure altitude of 3,000 m, which corresponds to an angle of attack of 12.4°. The state vector is

$$x = [\alpha \quad \beta \quad p \quad q \quad r]^T \tag{35}$$

where α is the angle of attack (rad), β is the sideslip angle (rad), p is the roll rate (rad/s), q is the pitch rate (rad/s), and r is the yaw rate (rad/s). The control vector is $u = [\delta_c \quad \delta_{r_e} \quad \delta_{l_e} \quad \delta_r]^T$, which represents the angular deflections of the canards (rad), right elevon (rad), left elevon (rad), and rudder (rad). Straight-level flight at this operation point demands 6° of deflection in both elevons, and approximately 0° of canard deflection.

The related continuous-time linear model matrices are [30]

$$A = \begin{bmatrix} -0.5432 & 0.01370 & 0 & 0.9778 & 0 \\ 0 & -0.1179 & 0.2215 & 0 & -0.9661 \\ 0 & -10.51 & -0.9967 & 0 & 0.6176 \\ 2.622 & -0.0030 & 0 & -0.5057 & 0 \\ 0 & 0.7075 & -0.0939 & 0 & -0.2127 \end{bmatrix} \tag{36}$$

$$B = \begin{bmatrix} 0.0069 & -0.0866 & -0.0866 & 0.0004 \\ 0 & 0.0119 & -0.0119 & 0.0287 \\ 0 & -4.242 & 4.242 & 1.487 \\ 1.653 & -1.274 & -1.274 & 0.0024 \\ 0 & -0.281 & 0.281 & -0.882 \end{bmatrix} \tag{37}$$

The performance output expressed by Eq. (17) is defined by $w = x$, and is required to follow the model given by

$$A_m = \begin{bmatrix} -0.7113 & 0.01260 & 0 & 0.8809 & 0.0006 \\ 0 & -0.1357 & 0.2228 & 0 & -0.9311 \\ -0.01380 & -9.143 & -2.910 & -0.00741 & 1.362 \\ -1.497 & -0.0270 & -0.00141 & -2.902 & 0.00728 \\ 0.0030 & 1.214 & -0.100 & 0.00162 & -1.269 \end{bmatrix} \tag{38}$$

where A_m has eigenvalues $\{-0.989 \pm 1.402i \quad -1.807 \pm 3.45i - 2.338\}$. The weight matrices Q and R of Eq. (22) were set to $Q = I$ and $R = 10^{-10} I$. The dynamic system and the weight matrices were discretized with $T_s = 0.1$ s, which the matrices Φ, Γ, Q_d, W_d and R_d are obtained, along with the feedback gain:

$$K_d = \begin{bmatrix} 1.0754 & 0.006974 & 0.00055 & 0.6294 & -0.001422 \\ -0.8014 & 0.3065 & -0.1733 & -0.4718 & -0.1282 \\ -0.8014 & 0.3065 & -0.1733 & -0.4718 & -0.1282 \\ 0.003447 & 0.3082 & 0.1192 & 0.001892 & -1.076 \end{bmatrix} \tag{39}$$

The target calculation problem assumes that the controlled variables are $z = [\alpha \quad \beta \quad p]^T$ expressed in degrees and degrees per second, and that the full state is observed. Along with Eq. (1), these assumptions lead to $E = I$ and

$$H = \begin{bmatrix} 57.3 & 0 & 0 & 0 & 0 \\ 0 & 57.3 & 0 & 0 & 0 \\ 0 & 0 & 57.3 & 0 & 0 \end{bmatrix} \tag{40}$$

The weights from Eq. (4) were set to $Q_{ss} = I$ and $R_{ss} = 1 \times 10^{-10} I$. The disturbance model was chosen to have three variables and the related distribution matrix Γ_d was built from the first three columns of Γ. The disturbance vector was bounded between values $\pm[1 \quad 1 \quad 1]$ rad. The observer gain L was obtained by first computing L_x and after $\bar{L}_d$, through the LQR technique.

The proposed numerical example was implemented in the MATLAB environment. The constrained feasible target problem and the implicit model following regulator were solved through the active set method of Goldfarb and Idnani [32].

A. Case 1: Canard Jammed at 25°

The first fault case considers a severe failure of the canard, which remains stuck in its full positive angular position of 25°. Under nominal conditions, the set of admissible controls was considered to be $-55° \leq \delta_c \leq 25°$, $-30° \leq \delta_{r_e} \leq 30°$, $-30° \leq \delta_{l_e} \leq 30°$ and $-30° \leq \delta_r \leq 30°$ [29,30]. In this faulty situation, the constraints on the aerodynamic surface have changed, i.e., the constraints over the canard are modified to $24.95° \leq \delta_c \leq 25°$.

Algorithm 1 Set of statically admissible commands $\mathbf{P}_m$

Require: matrix L_{ss}, vector k_{ss} for the fault case
create polyhedron $\mathbf{P}_{ss}$ as indicated in Eq. (10)
generate polyhedron $\mathbf{P}_w$ through projection $\pi_{\mathbb{W}} \mathbf{P}_{ss}$
Require: estimated $\hat{d}_k$
generate polyhedron $\mathbf{P}_m$ through slice $\sigma_{\hat{d}_k} \mathbf{P}_w$

The statically admissible sets in both the nominal and fault case were obtained by following Algorithm 1 of Sec. II through numerical methods [33] and are shown in Fig. 4, considering the disturbance vector to be zero. A constraint of $0.4° \leq \alpha \leq 22.4°$ is considered herein, simply to establish practical bounds over the admissible sets. The right side of Fig. 4 shows the related polyhedra sliced at zero commanded sideslip angle. Clearly, under faulty condition, the ability of the aircraft to roll at positive angles of attack is compromised. The steady-state roll rate is reduced as larger angles of attack are demanded because both elevons are responsible for counteracting the effect of the jammed canard and are also employed to track the angle of attack. Note that the maximum steady-state value of the angle of attack, under these trimmed conditions, is 21.6°, which corresponds to the right vertex of the maneuverability polyhedron.

The proposed reference management method was applied to filter the demands (r_c) on the angle of attack, sideslip angle and roll rate. The selected MPC control horizon was $N = 2$. A simulation was performed in which the aircraft was required to increase its angle of attack to 22.4°, followed by a roll demand of 150°/s and return to the initial angle of attack. Figure 5 presents the related admissible (r_{ss}) and feasible ($z_{ss} = HEx_{ss}$) command values. Because the maximum commandable angle of attack is 21.6°, the demanded value of 22.4° was not achievable. If the commanded angle of attack is reduced to 12.4°, the aircraft is capable of tracking a range of roll rates but cannot achieve the required 150°/s. Hence, both the commanded angle of attack and roll rate were filtered, considering the airframe's capability to stabilize under those new conditions with the available aerodynamic surfaces.

The second filtering process transforms the admissible command (r_{ss}) into the feasible command (z_{ss}), taking into account the current estimated values of the state and disturbance vectors. Reducing the angle of attack while also tracking a positive value of roll rate was a demanding task to both the elevons and the rudder. As shown in Fig. 5, the roll rate and the angle of attack were gradually increased and decreased, respectively. At the same time, some sideslip angle was commanded, because the rudder was also applied in this maneuver. At steady state, the feasible commands coincided with the admissible command.

Figure 6 shows the time responses of the tracking variables. It is worthy noting the offset-free capability of the MPC controller in all

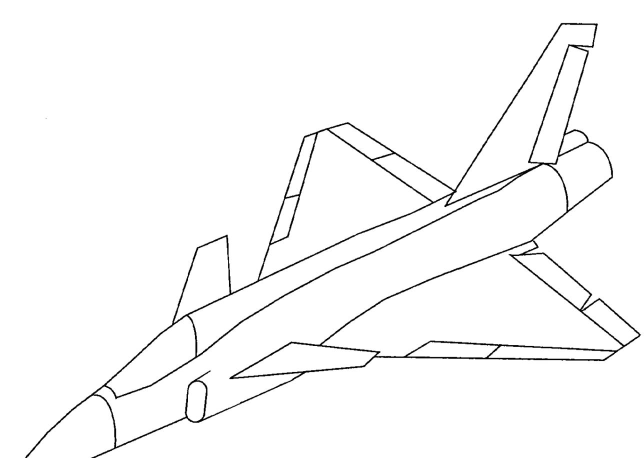

Fig. 3 ADMIRE view.

Algorithm 2 Set of admissible steady-state values $\mathbf{X}_{ss_N}$

Require: state, input and disturbance constraints for the fault case
compute invariant set $O_\infty(x_{ss}, u_{ss})$ of the extended dynamic model Eq. (12)
generate polyhedron $\mathbf{X}_N$ through recursion and projection
Require: estimated state and disturbance vectors $(\hat{d}_k, \hat{x}_k)$
generate polyhedron $\mathbf{X}_{ss_N}$ through slice $\sigma_{(\hat{x}_k, \hat{d}_k)}\mathbf{X}_N$

variables with respect to the admissible command, despite the severe canard fault. The aerodynamic surfaces deflections are presented in Fig. 7. During the tracking of the angle of attack, both elevons were deflected at their maximum values, characterizing the right vertex of the maneuverability polyhedron. Note also that the rudder twice moves to its limit of $-30°$ during the demand level modification.

B. Case 2: Right Elevon Jammed at −14°

In the second fault case, the right elevon was jammed at angular position $-14°$. Figure 8 shows the sets of statically admissible commands in the nominal and faulty scenarios for zero disturbance. The capability of the fighter to acquire negative roll rates is jeopardized by the strong positive rolling moment created by the stuck aerodynamic surface.

Maintaining the same control horizon $N = 2$ used in the last example, a linear nominal simulation was conducted with an abrupt change of demand in roll from $+200$ to $-200°/\text{s}$. As it can be seen in Fig. 9, those demand levels are not admissible, but the reference management filters the command and provides roll demands that are compatible with the faulty airframe. The feasible and admissible roll commands are similar, but both the feasible commands for both angle of attack and sideslip differ from the admissible values. This happens because the roll reversal requires full left elevon deflection, which in turn generates more pitching moment than the canard can counteract. To maintain the feasibility of the model predictive controller, an abrupt change in the angle of attack is demanded. The same occurs to the transient sideslip excursion after rudder saturation.

Figure 10 presents the time responses of the tracked variables. Despite the transient motion during the roll reversal, the MPC controller was able to track the feasible commands without offset. The aforementioned saturation of the control surfaces is showed in Fig. 11. Fifteen seconds into the simulation, the roll reversal is executed, pushing all control signals to their limits. It is worthy to note that the left elevon assumes full positive deflection with the positive roll rate command and full negative deflection with the negative roll rate command, thus defining the maximum and minimum values of a statically admissible roll command.

C. Case 3: Loss of Effectiveness in the Left Elevon

To demonstrate the ability of the reference management method to deal with unknown failures, a loss of 80% of the control effectiveness in the right elevon along with the right elevon stuck at $-14°$ is simulated. The FDI functionality of the Fig. 2 cannot detect the loss

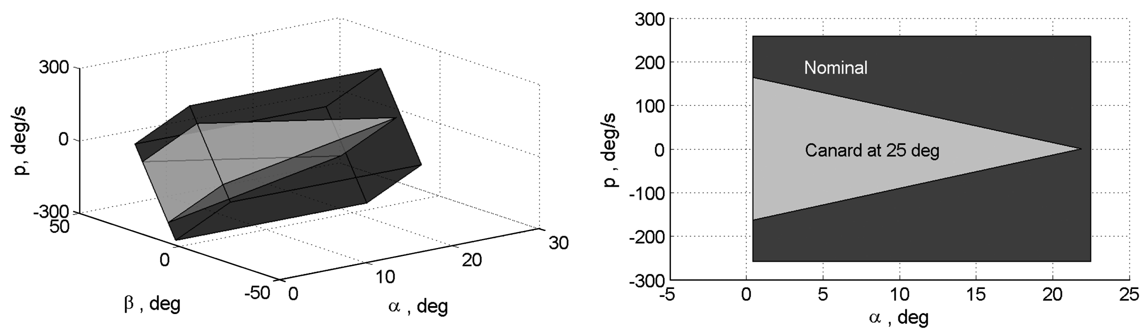

Fig. 4 Statically admissible sets (nominal and canard fault cases) and their slice at zero sideslip angle.

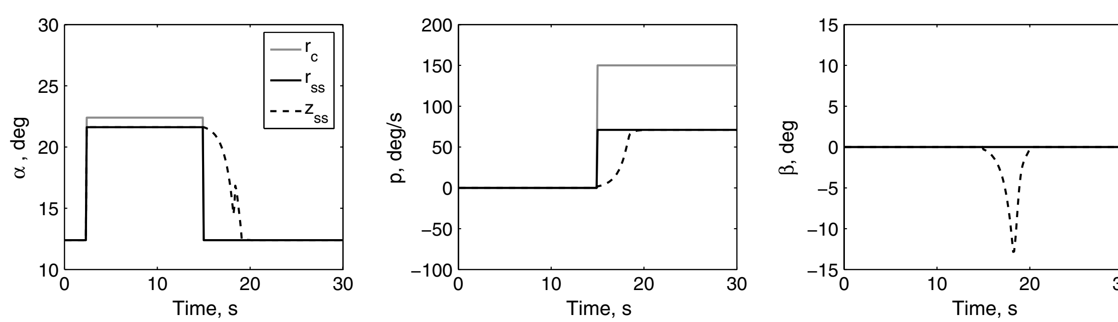

Fig. 5 Statically admissible and feasible command values in fault case 1.

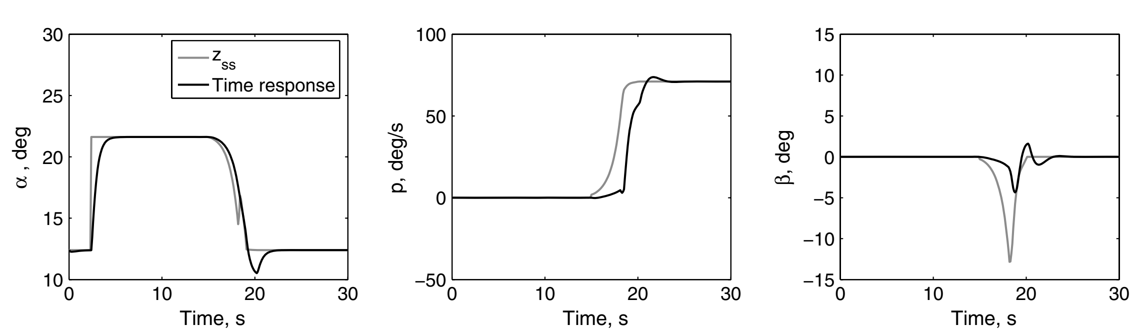

Fig. 6 Evolution of the aircraft model states in fault case 1.

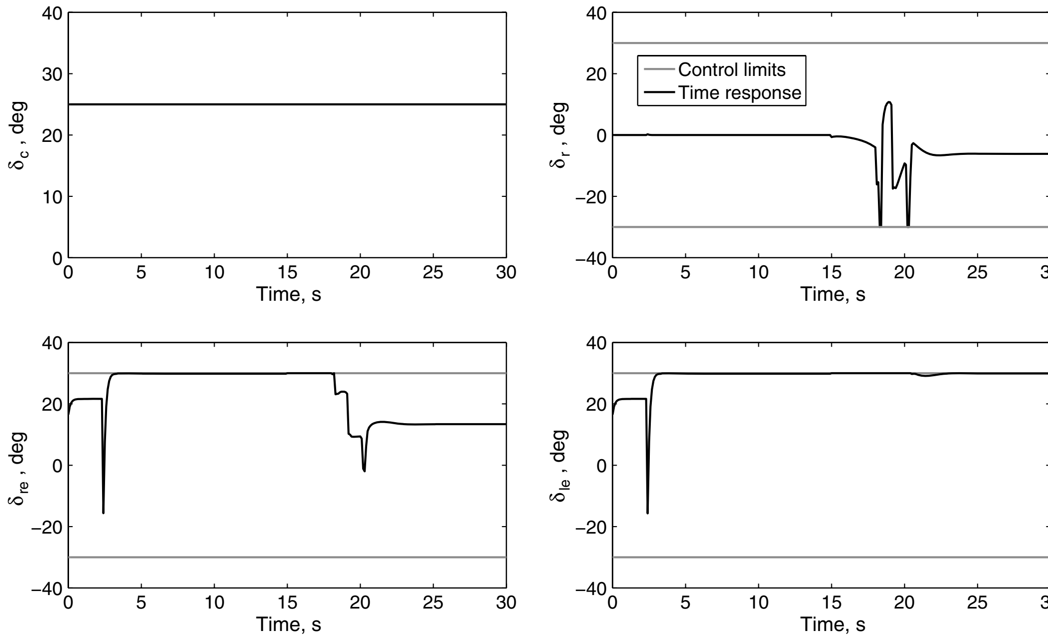

Fig. 7 Evolution of the aircraft model inputs in fault case 1.

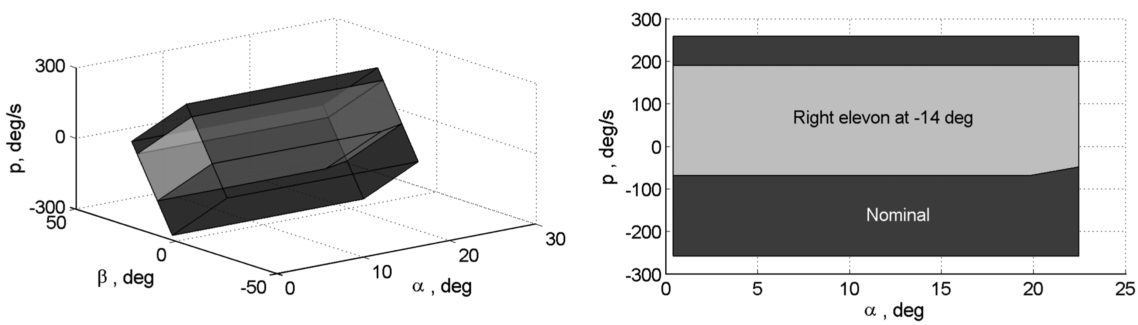

Fig. 8 Statically admissible sets (nominal and right elevon fault cases) and their slice at zero sideslip angle.

of effectiveness, but the observer enclosed by the model predictive controller is designed to capture the plant-model mismatch caused by the damaged surface by estimating the disturbance vector. Hence, the admissible and feasible command values rely on the estimated disturbance vector, as defined by Algorithm 1. Instead of the time-invariant maneuverability polyhedron of the previous examples, the estimated disturbance changes the shape of the statically admissible command set at each sampling time.

Figure 12 presents the admissible and feasible commands under the same conditions and demands of the last example. The reference management functionality was able to identify the reduced maneuverability caused by the two faults (right and left elevons), considerably reducing the maximum absolute values of the roll rate. The aircraft can now hardly roll to the left, and most of the admissible positive roll rate command is due to the stuck right elevon. To guarantee feasibility of the MPC numerical problem, some sideslip angle was demanded along with the negative roll rate command.

The time histories of the estimated states and controls are presented in Figs. 13 and 14. No offset is observed, with respect to the feasible commands, demonstrating the ability of the observer to deal with plant-model mismatch. Figure 15 shows the estimated disturbance values during the simulation. For each feasible command, the disturbances are properly estimated with satisfactory dynamic response.

D. Case 4: Right and Left Elevon Jammed at 6°

Finally, a double fault scenario is considered in which both elevons are jammed in the trimmed position 6°. Figure 16 shows the resulting degenerated maneuverability polyhedron (without disturbances).

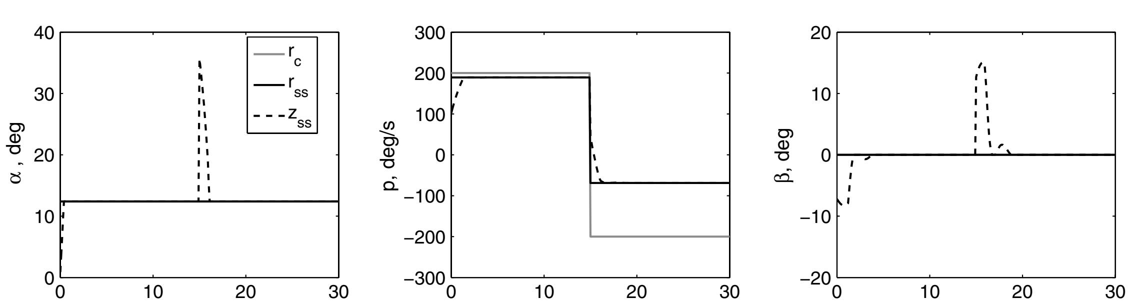

Fig. 9 Statically admissible and feasible command values in fault case 2.

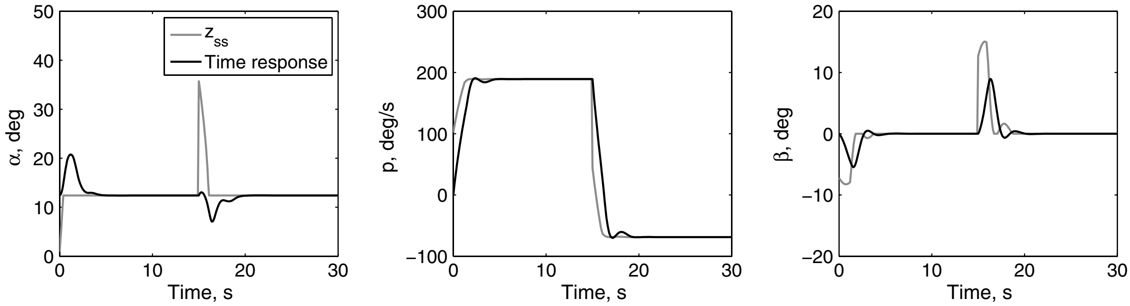

Fig. 10 Evolution of the aircraft model states in fault case 2.

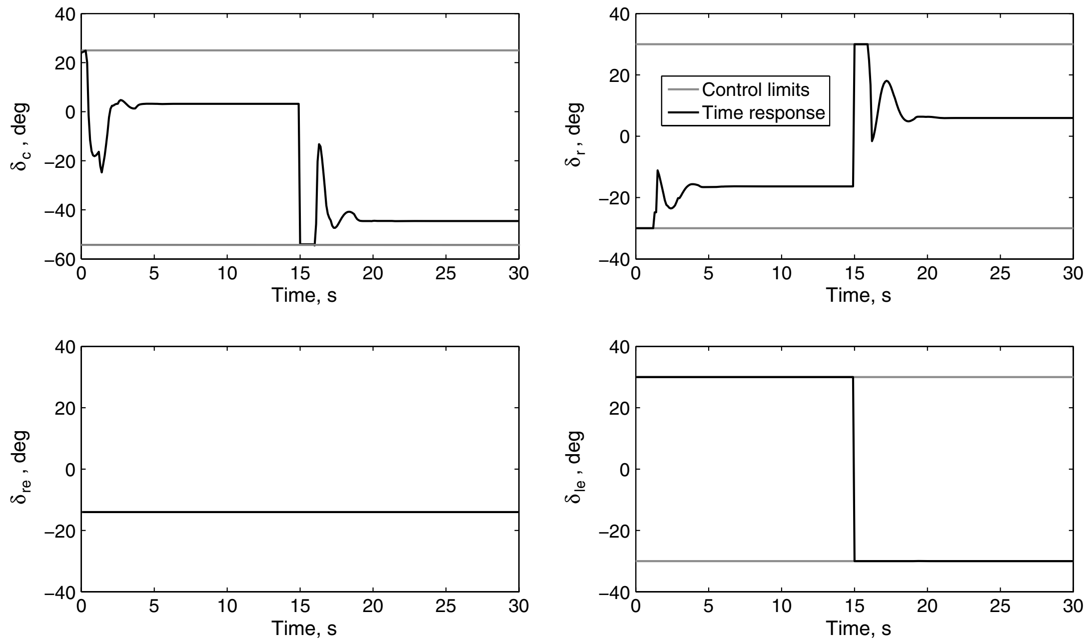

Fig. 11 Evolution of the aircraft model inputs in fault case 2.

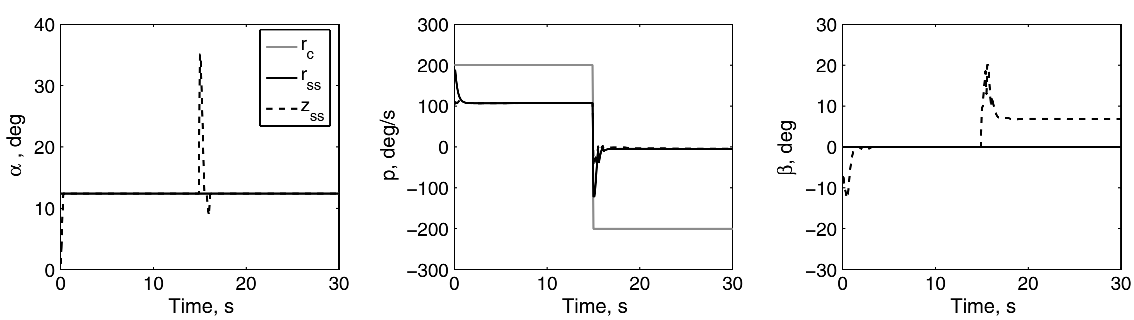

Fig. 12 Statically admissible and feasible command values in fault case 3.

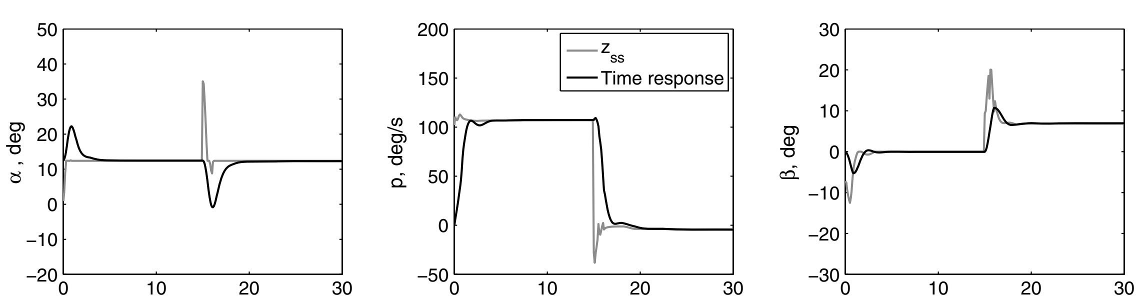

Fig. 13 Evolution of the aircraft model states in fault case 3.

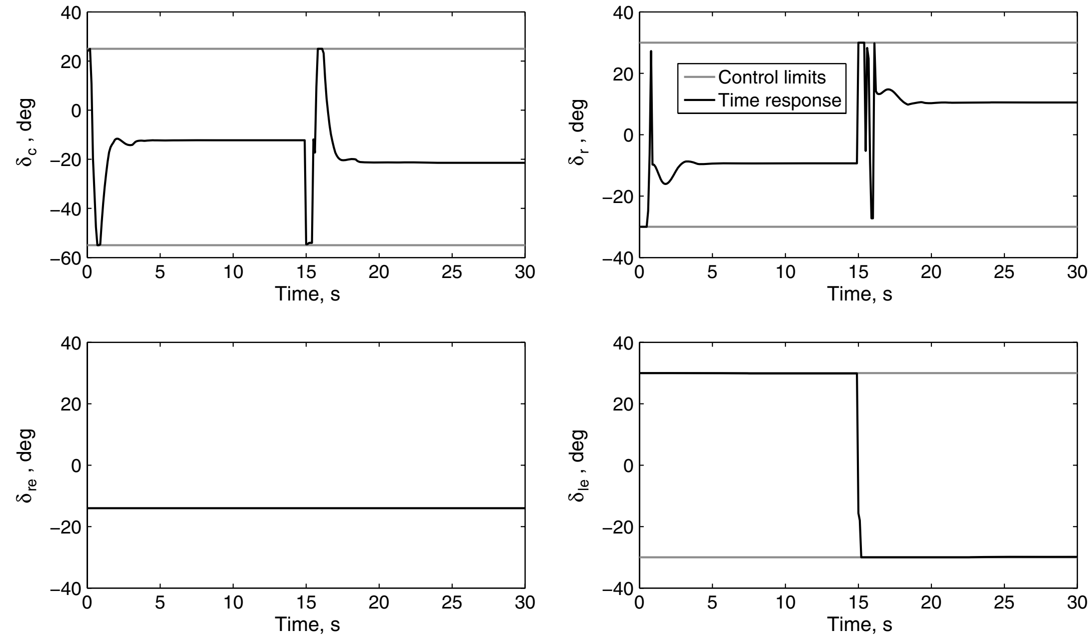

Fig. 14 Evolution of the aircraft model inputs in fault case 3.

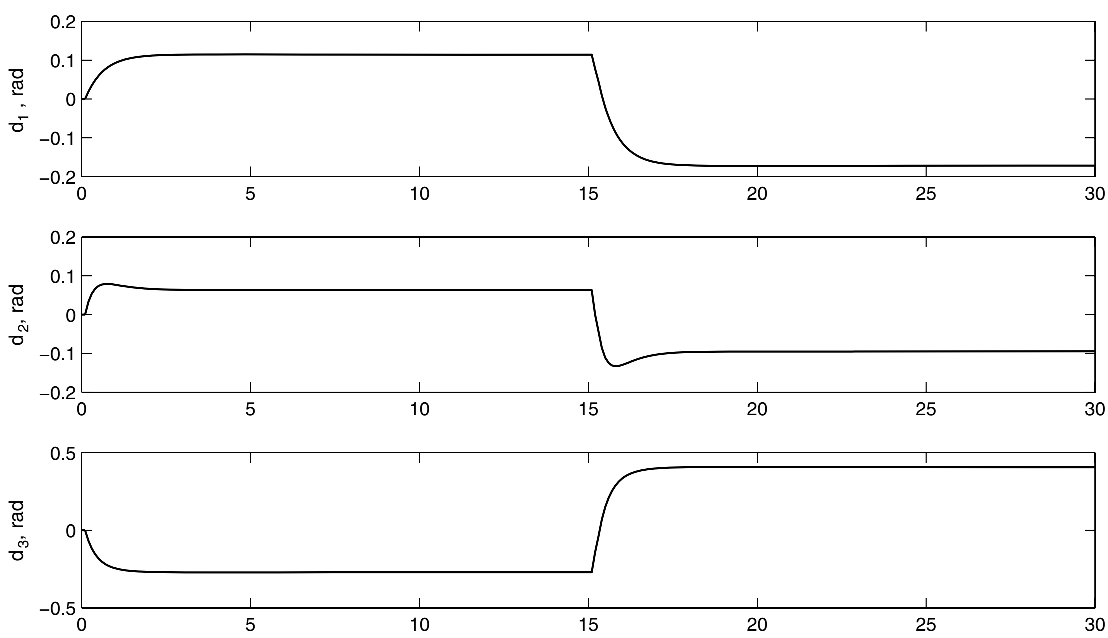

Fig. 15 Evolution of the estimated disturbance vector elements in fault case 3.

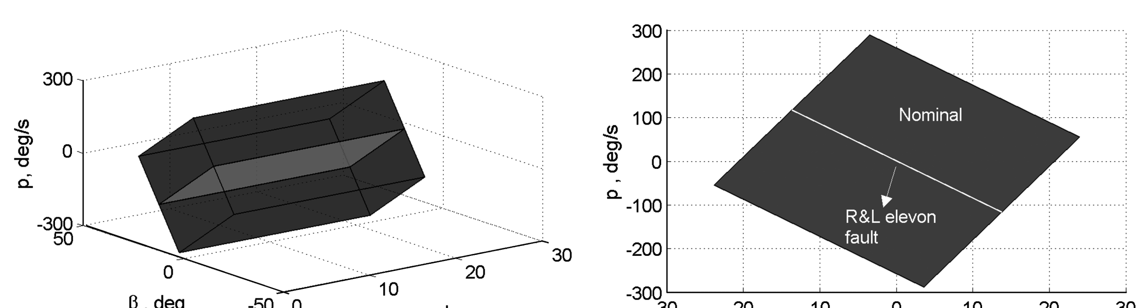

Fig. 16 Statically admissible sets (nominal and double elevons fault cases) and their slice at the trimmed angle of attack.

It is only possible to achieve roll rates by also varying the sideslip angle, and vice-versa because the rudder is the sole aerodynamic surface that can control the roll movement. The roll is accomplished by generating sideslip, which makes the aircraft roll through the dihedral effect. Figure 16 shows the following proportional relationship between the admissible levels of the roll rate and the sideslip angle:

$$\beta_{ss} = -0.1192 p_{ss} \tag{41}$$

Setting control horizon to $N = 2$ for the model predictive controller, the admissible and feasible commands, for a roll reversal maneuver from $+20$ to $-20°/\mathrm{s}$, are presented in Fig. 17. Clearly the computed feasible commands are slower than the related admissible values because the rudder alone is responsible to track both roll rate and sideslip angle.

Although only one aerodynamic surface remains to track the two variables, the admissible commands computed through Eq. (41) assures that offset will not occur in steady state, as can be seen in Fig. 18. Because both elevons are jammed in the trimmed position, the roll reversal maneuver develops without disturbing the longitudinal axis. Thus, Fig. 19 only shows displacements in the rudder deflection.

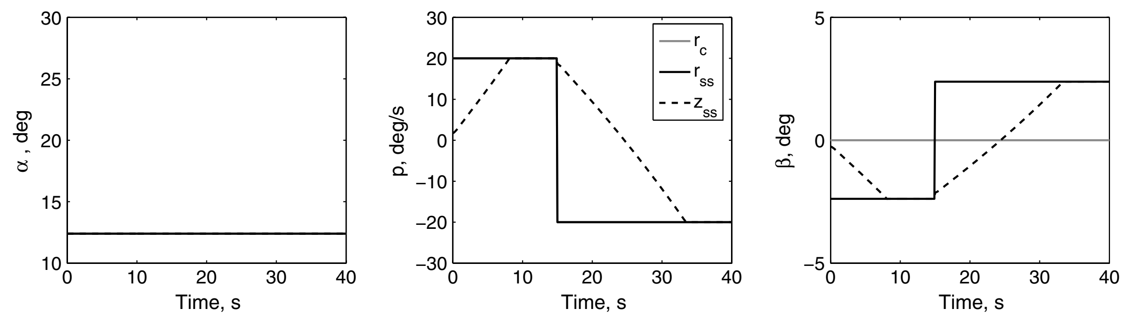

Fig. 17 Statically admissible and feasible command values in fault case 4.

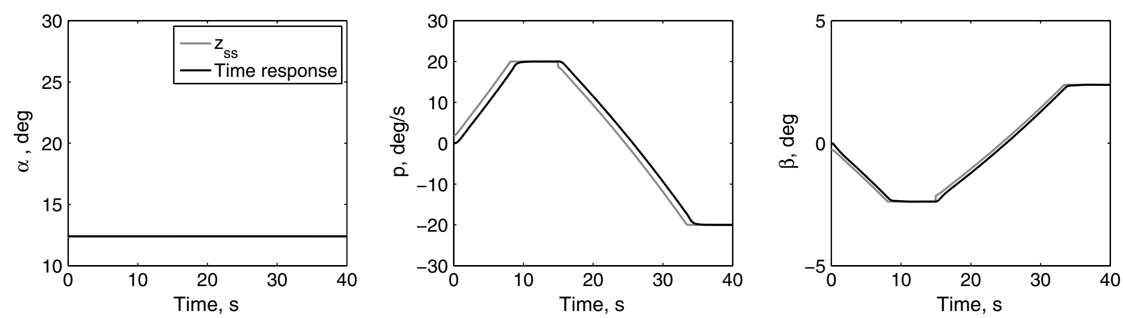

Fig. 18 Evolution of the aircraft model states in fault case 4.

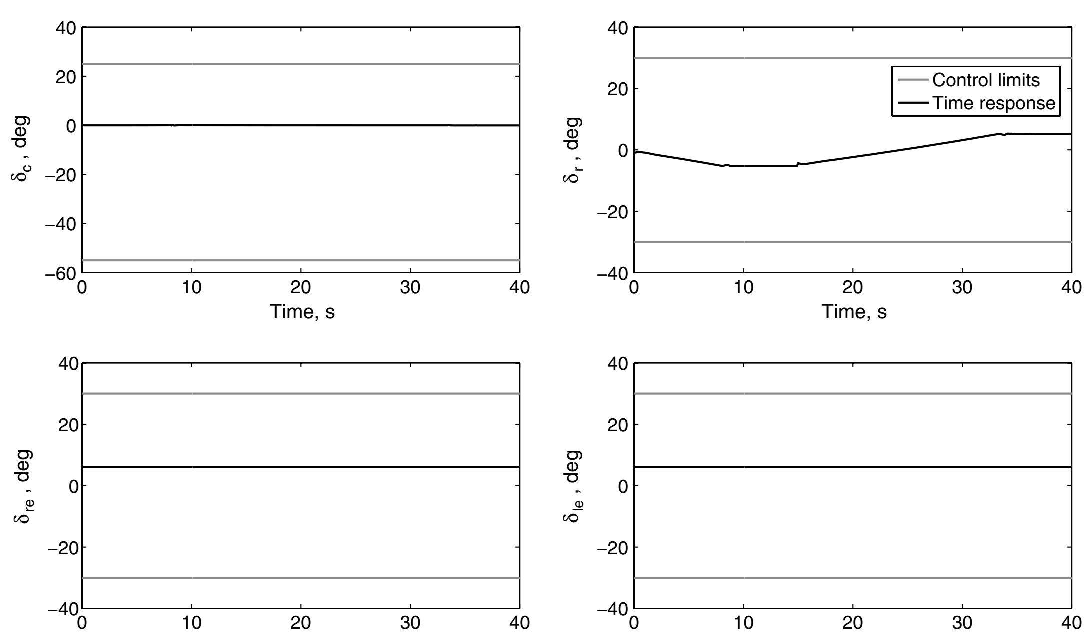

Fig. 19 Evolution of the aircraft model inputs in fault case 4.

Table 1 Fault-tolerant controller computation times

Criterion	Case 1	Case 3	Case 4
Max. time, ms	18.8	15.6	13.5
Min. time, ms	4.18	3.55	4.86
Avg. time, ms	6.10	6.20	6.10

E. Computational Burden Analysis

Table 1 shows some data on the computational demands of the proposed reference management technique, using the CPU-time routine in MATLAB. The simulations were conducted on a PC with Intel Core 2 Duo technology.

The maximum computation times are compatible with the considered sampling rate (100 ms), and the average times are lower than those obtained in a PC environment by Kale and Chipperfield [12] with a fault-tolerant model predictive controller (40–55 ms) and by Famularo et al. [10] with a reference governor strategy (14–18 ms). Although the proposed controller comprises two QP solvers, the feasible target calculator computes the state and control vectors in steady state in a way that alleviates the computational load on the second solver, related to the constrained implicit model following regulator. In MPC, the second solver typically takes more time to obtain a feasible constrained solution. With the proposed modification to the first QP problem, the second QP solver handles a smoother constrained optimization problem. Moreover, the feasible target calculator always provides reachable values to the constrained regulator for any control horizon N. Thus, the traditional way of enlarging the domain of operation of MPC controllers is avoided, and large control horizons are no longer required. This is clearly an advantage in applications in which computational power is restricted or when the control of fast dynamic modes requires small sampling rates.

V. Conclusions

The design of flight control systems with tolerance against several types of faults is a challenging task. The controller must be able to redistribute the control signals among the remaining actuators. Additionally, the reduced maneuverability of the damaged aircraft must be taken into account when computing the new equilibrium conditions and the dynamic behavior to steer the current state to a new trimmed position. Depending on the severity of the fault, closed-loop stability can be seriously compromised. In this paper, a new reference management method for fault-tolerant control has been proposed to solve such problems. The presented technique combines one scheme concerned with the physical admissibility of steady-state values (airframe limitations) with another designed to guarantee feasibility and stability in the constrained controller. MPC was considered, given its ability to perform control redistribution.

The proposed reference management technique has been applied in numerical examples of a fighter aircraft. Various critical actuator faults were considered and aggressive maneuvers were demanded. The reference management method was able to filter the demands in both static and dynamic ways. Given the feasible demands, the model predictive controller was capable of maintaining feasibility during maneuvers, without any tracking error in the new steady state, with very little computational burden.

In future research, it would be interesting to move the reference management device to the outer control loops in which the demands are generated. Additionally, further investigations are necessary to explore the fault-tolerant characteristics of the employed linear observer for offset-free tracking against various cases of airframe structural faults.

Acknowledgment

The author would like to acknowledge Karl Kienitz (Instituto Tecnológico de Aeronáutica Brazil) for his scientific assistance and cooperation.

References

[1] Strube, M., Sanner, R., and Atkins, E., "Dynamic Flight Guidance Recalibration After Actuator Failures," AIAA First Intelligent Systems Technical Conference, AIAA Paper 2004-6255, Chicago, Sept. 2004.

[2] Ducard, G., Kulling, K., and Geering, H., "Evaluation of Reduction in the Performance of a Small UAV After an Aileron Failure for an Adaptive Guidance System," *Proceedings of the 2007 American Control Conference*, New York, July 2007, pp. 1793–1798.

[3] Kapasouris, P., Athans, M., and Stein, G., "Design of Feedback Control Systems for Stable Plants with Saturating Actuators," *Proceedings of the 27th IEEE Conference on Decision and Control*, Austin, TX, 1988, pp. 469–479.

[4] Gilbert, E., and Tan, K., "Linear Systems with State and Control Constraints: The Theory and Application of Maximal Output Admissible Sets," *IEEE Transactions on Automatic Control*, Vol. 36, No. 9, 1991, pp. 1008–1020.
doi:10.1109/9.83532

[5] Gilbert, E., and Kolmanovski, I., "Discrete-Time Reference Governors and the Nonlinear Control of Systems with State and Control Constraints," *International Journal of Robust and Nonlinear Control*, Vol. 5, No. 5, 1995, pp. 487–504.
doi:10.1002/rnc.4590050508

[6] Gilbert, E., and Kolmanovski, I., "Fast Reference Governors for Systems with State and Control Constraints and Disturbance Inputs," *International Journal of Robust and Nonlinear Control*, Vol. 9, No. 15, 1999, pp. 1117–1141.
doi:10.1002/(SICI)1099-1239(19991230)9:15<1117::AID-RNC447>3.0.CO;2-I

[7] Casavola, A., Mosca, E., and Angeli, D., "Robust Command Governors for Constrained Linear Systems," *IEEE Transactions on Automatic Control*, Vol. 45, No. 11, 2000, pp. 2071–2077.
doi:10.1109/9.887628

[8] Angeli, D., and Mosca, E., "Command Governors for Constrained Nonlinear Systems," *IEEE Transactions on Automatic Control*, Vol. 44, No. 4, 1999, pp. 816–820.
doi:10.1109/9.754825

[9] Gilbert, E., and Kolmanovski, I., "Nonlinear Tracking Control in the Presence of State and Control Constraints: A Generalized Reference Governor," *Automatica*, Vol. 38, No. 12, 2002, pp. 2063–2073.
doi:10.1016/S0005-1098(02)00135-8

[10] Famularo, D., Martino, D., and Mattei, M., "Constrained Control Strategies to Improve Safety and Comfort on Aircraft," *Journal of Guidance, Control, and Dynamics*, Vol. 31, No. 6, Nov.–Dec. 2008, pp. 1782–1792.
doi:10.2514/1.34426

[11] Zhang, Y., and Jiang, J., "Fault Tolerant Control System Design with Explicit Consideration on Performance Degradation," *IEEE Transactions on Aerospace and Electronic Systems*, Vol. 39, No. 3, 2003, pp. 838–848.
doi:10.1109/TAES.2003.1238740

[12] Kale, M., and Chipperfield, A., "Stabilized MPC Formulations for Robust Reconfigurable Flight Control," *Control Engineering Practice*, Vol. 13, No. 6, 2005, pp. 771–788.
doi:10.1016/j.conengprac.2004.09.001

[13] Luo, Y., Serrani, A., Yurkovich, S., Oppenheimer, M. W., and Doman, D. B., "Model-Predictive Dynamic Control Allocation Scheme for Reentry Vehicles," *Journal of Guidance, Control, and Dynamics*, Vol. 30, No. 1, Jan.–Feb. 2007, pp. 100–113.
doi:10.2514/1.25473

[14] Miksch, T., Gambier, A., and Badreddin, E., "Real-Time Implementation of Fault-Tolerant Control Using Model Predictive Control," *Proceedings of the 17th IFAC World Congress*, Seoul, Korea, July 2008, pp. 11136–11141.

[15] de Almeida, F., *Trajectory Tracking with Fault-Tolerant Flight Control System: A Model Predictive Control Approach*, Shaker, Aachen, Germany, 2009, Chap. 4.

[16] Chisci, L., and Zappa, G., "Dual Mode Predictive Tracking of Piecewise Constant References for Constrained Linear Systems," *International Journal of Control*, Vol. 76, No. 1, 2003, pp. 61–72.
doi:10.1080/0020717021000049160

[17] Limon, D., Alvarado, I., Alamo, T., and Camacho, E. F., "MPC for Tracking Piecewise Constant References for Constrained Linear Systems," *Automatica*, Vol. 44, No. 9, 2008, pp. 2382–2387.
doi:10.1016/j.automatica.2008.01.023

[18] Limon, D., Alvarado, I., Alamo, T., and Camacho, E. F., "Robust Tube-Based MPC for Tracking of Constrained Linear Systems with Additive Disturbances," *Journal of Process Control*, Vol. 20, No. 3, 2010,

pp. 248–260.
doi:10.1016/j.jprocont.2009.11.007

[19] de Almeida, F., and Leissling, D., “Fault-Tolerant Flight Control System Using Model Predictive Control,” *Proceedings of the Third CTA-DLR Workshop on Data Analysis and Flight Control*, Proc. No. 58836, São José dos Campos, Brazil, Sept. 2009.

[20] Jones, C., Kerrigan, E., and Maciejowski, J., “On Polyhedral Projection and Parametric Programming,” *Journal of Optimization Theory and Applications*, Vol. 138, No. 2, April 2008, pp. 207–220.
doi:10.1007/s10957-008-9384-4

[21] de Almeida, F., and Leissling, D., “Fault-Tolerant Model Predictive Control with Flight-Test Results,” *Journal of Guidance, Control, and Dynamics*, Vol. 33, No. 2, March–April 2010, pp. 363–375.
doi:10.2514/1.46108

[22] Maeder, U., Borrelli, F., and Morari, M., “Linear Offset-Free Model Predictive Control,” *Automatica*, Vol. 45, No. 10, Oct. 2009, pp. 2214–2222.
doi:10.1016/j.automatica.2009.06.005

[23] Bryson, A., *Control of Spacecraft and Aircraft*, Princeton Univ. Press, Princeton, NJ, 1994, Appendix D.

[24] Loan, C., “Computing Integrals Involving the Matrix Exponential,” *IEEE Transactions on Automatic Control*, Vol. 23, No. 3, 1978, pp. 395–404.
doi:10.1109/TAC.1978.1101743

[25] Rossiter, J., Kouvaritakis, B., and Rice, M., “A Numerically Robust State-Space Approach to Stable-Predictive Control Strategies,” *Automatica*, Vol. 34, No. 1, 1998, pp. 65–73.
doi:10.1016/S0005-1098(97)00171-4

[26] Mayne, D., Rawlings, J., Rao, C., and Scokaert, P., “Constrained Model Predictive Control: Stability and Optimality,” *Automatica*, Vol. 36, No. 6, 2000, pp. 789–814.
doi:10.1016/S0005-1098(99)00214-9

[27] Rossiter, J. A., *Model-Based Predictive Control: A Practical Approach*, CRC Press, Boca Raton, FL, 2003, Chap. 4.

[28] Forsell, L., and Nilsson, U., “ADMIRE the Aero-Data Model in a Research Environment Version 4.0, Model Description,” TR FOI-R-1624-SE, Swedish Defence Agency, Stockholm, Dec. 2005.

[29] Alwi, H., and Edwards, C., “Fault Tolerant Control Using Sliding Modes with On-Line Control Allocation,” *Automatica*, Vol. 44, No. 7, July 2008, pp. 1859–1866.
doi:10.1016/j.automatica.2007.10.034

[30] Harkegard, O., and Glad, S., “Resolving Actuator Redundancy: Optimal Control vs. Control Allocation,” *Automatica*, Vol. 41, No. 1, 2005, pp. 137–144.
doi:10.1016/S0005-1098(04)00255-9

[31] Kale, M., and Chipperfield, A., “Robust and Stabilized MPC Formulations for Fault Tolerant and Reconfigurable Flight Control,” *Proceedings of the IEEE International Symposium on Intelligent Control*, Taipei, Taiwan, Sept. 2004, pp. 222–227.

[32] Goldfarb, D., and Idnani, A., “A Numerically Stable Dual Method for Solving Strictly Convex Quadratic Programs,” *Mathematical Programming*, Vol. 27, No. 1, Sept. 1983, pp. 1–33.
doi:10.1007/BF02591962

[33] Kvasnica, M., *Real-Time Model Predictive Control via Multi-Parametric Programming: Theory and Tools*, 1st ed., VDM, Saarbrucken, Germany, 2009, Chap. 1.